IEEE Access
Multidisciplinary ⋮ Rapid Review ⋮ Open Access Journal

Received 25 June 2023, accepted 9 July 2023, date of publication 13 July 2023, date of current version 19 July 2023.

Digital Object Identifier 10.1109/ACCESS.2023.3295125

RESEARCH ARTICLE

Dynamic Frequency Assignment for Cognitive Radio Cellular Networks Using Hysteretic Noisy Chaotic Neural Network

CHENGZHI ZHAO AND AO ZHANG
School of Electronics Information, Yangtze University, Jingzhou, Hubei 434000, China

Corresponding author: Chengzhi Zhao (500177@yangtzeu.edu.cn)

This work was supported by the National Natural Science Foundation of China General Project "Performance Analysis and Optimal Design of Networked Intelligent Systems under Multiple Communication Constraints" under Grant 62173049.

ABSTRACT This paper presents a novel dynamic frequency assignment (DFA) technique for cognitive radio cellular networks (CRCNs) using hysteretic noisy chaotic neural network (HNCNN). HNCNN is a novel neural network that combines the advantages of stochastic chaotic simulated annealing and hysteretic dynamics to achieve performance improvements in dynamic frequency assignment. In DFA technique, an existing energy function is introduced, which avoids causing harmful interference to primary users (PUs) according to the real-time interference frequency table. In a CRCN, the introduced energy function also avoids causing mutual interferences among cells, considers the number of required frequencies for each cell, and simultaneously minimizes the total number of assigned frequencies to improve spectrum utilization. In the end, a typical 49-cell CRCN with 70 licensed frequencies is examined to demonstrate the validity of the proposed technique. And the results also show that HNCNN outperforms noisy chaotic neural network (NCNN) according to convergence speed and the rate of optimal solution.

INDEX TERMS Cognitive radio cellular networks, dynamic frequency assignment, energy function, interference frequency table, hysteretic noisy chaotic neural network.

I. INTRODUCTION

The existing spectrum allocations policy has been shown that the spectrum is not utilized efficiently in licensed spectrum [1]. Cognitive radio offers a flexible spectrum access technique paradigm, which was firstly proposed by Mitola [2]. In cognitive radio scenario, the unlicensed users (secondary users or cognitive users) could sense a vacant spectrum which is unoccupied by licensed users (primary users) [3], and are permitted to "borrow" the vacant spectrum from the licensed spectrum opportunistically.

As an intelligent wireless communication system [4], cognitive radio contains two key research challenges which are spectrum sensing and dynamic spectrum access (DSA) [5], which is called dynamic frequency assignment (DFA) in our research. Spectrum sensing requires secondary users (SUs) to sense spectrum of primary users (PUs), and DFA demands SUs to access the vacant spectrum without causing harmful interference to PUs [6].

DFA technique is closely related to the cognitive radio network architecture. In previous works, typical network architecture of cognitive radio includes Wireless Region Area Network (WRAN) [1], mobile ad hoc network [7], wireless mesh network [8], and cognitive radio cellular network (CRCN) [9], In [10], a spectrum-aware and energy-aware operation scheme for cellular networks in a cognitive radio context is proposed.

Among all the network architectures mentioned above, cellular network is not only a perfect paradigm for mobile communications, but also a promising wireless access technology for cognitive radio [11]. However, when a traditional cellular network is applied to cognitive radio, the available frequencies (unoccupied by PUs) are not fixed and constantly change over time from one region to another. So the DFA problem for a CRCN becomes more complicated than

The associate editor coordinating the review of this manuscript and approving it for publication was Tiankui Zhang.

dynamic channel assignment (DCA) for the traditional cellular networks [12], [13].

Therefore, in a CRCN, how to dynamically assign the required frequencies to each cell according to the unoccupied frequencies information, and simultaneously avoid causing harmful interference to PUs, and mutual interference among cells. To the best of our knowledge, for the existing DSA schemes, there is no precious work has solved the problem successfully as yet.

In [9], Ma et al. proposed a DSA approach for CRCN, but the DSA process must be assisted by PUs, which is impractical in many cases. In [14], a two-phase channel and power allocation scheme is proposed for a cognitive radio network which consists of multiple cells, but the mutual interference among cells is hard to control. In [15], dynamic frequency allocation based on graph coloring and local bargaining for multi-cell WRAN system is proposed, but only the co-channel interference among cells is taken into account. In [16], Ahmed et al. proposed a CR-enabled IoT cellular network which composed of multiple PU base-stations, but there is no SU cellular network framework.

This paper presents a novel DFA technique for CRCNs using hysteretic noisy chaotic neural network (HNCNN).

In a CRCN, all cells are controlled by a central server, namely, spectrum broker, which is responsible for assigning available frequencies to cells. In a cell, both the base station (BS) and the related SUs are responsible for sensing the licensed spectrum, and then report the occupied spectrum information to the central server. Based on the occupied spectrum information of PUs in each cell, an interference frequency table is introduced for the CRCN.

Initially, each cell is assigned a frequency as the dedicated common control channel (such as a TDMA or a CDMA channel, or a set of sub-carriers of orthogonal frequency division multiplexing in a vacant frequency), which facilitates the BS to control and manage the related SUs. In each cell, the assigned common control channel will not to be switched to another vacant frequency unless it is occupied by PUs. When a new SU arrives in a cell, it first searches the common control channel and registers itself.

In order to avoid causing harmful mutual interference to PUs, DFA should avoid all interference frequencies in the interference frequency table. In addition, DFA should also avoid causing mutual interference among cells. Whenever a SU asks the BS for communicating, it will be assigned a channel (a frequency may service more than one SU), otherwise the SU will be blocked. Similarly, when a SU completes communication, the assigned frequency (or a channel) is released immediately and is available for other SUs.

Similar to the DCA for traditional cellular networks, DFA technique for CRCN is also a typical NP-hard problem with the existing solving schemes: simulated annealing, genetic algorithm, and neural network algorithm [17], [18]. Neural network is easy to be implemented by hardware and runs quickly. HNCNN [19] outperforms the noisy chaotic neural network (NCNN) [20], the transiently chaotic neural network (TCNN) [21] and the earlier Hopfield neural network (HNN) [22].

Whether an NP-hard problem can be successfully solved by HNCNN depends on a valid energy function, in which both constraints and optimizing objects are considered. The existing energy functions of DCA scheme [17], [18] for traditional cellular networks are not suitable for CRCNs, in which the available frequencies (unoccupied by PUs) are not fixed and constantly change over time from one region to another.

In [23], we proposed a novel energy function to solve the DCA problem using NCNN for large-scale cellular networks. In this paper, we introduce the proposed energy function in [23] to further solve the DFA problem for CRCNs. The introduced energy function avoids causing harmful interference to PUs according to the real-time interference frequency table, and considers the three mutual interference constraints among cells including co-site constraint (CSC), adjacent frequency constraint (AFC) and co-frequency constraint (CFC) [17], and the number of required frequencies of each cell. To improve spectrum utilization, the introduced energy function also minimizes the total number of assigned frequencies from the available ones.

The validity of the proposed DFA technique is confirmed by an instance of a 49-cell CRCN with 70 licensed frequencies.

II. ENERGY FUNCTION MODEL

A. HNCNN

Without increasing the number of adjustment parameters, Ming Sun et al. combined the advantages of both stochastic chaotic simulated annealing and hysteretic dynamics to obtain a novel HNCNN [19], [24] on the basis of NCNN [20]. Compared with NCNN and early HNN [22], the search capability and convergence speed of HNCNN are significantly improved. HNCNN is described as follows:

$$u_i(t+1) = k\left[u_i(t) + \eta_i(t)\right] + \alpha\left[\sum_{j=1}^{n} w_{ij}v_j(t) + b_i\right] - z_i(t)\left[v_i(t) - I_0\right] + n_i(t) \tag{1}$$

$$v_i = \frac{1}{1 + \exp\left\{-\left[u_i(t) + \eta_i(t)\right]/\varepsilon\right\}} \tag{2}$$

$$z_i(t) = (1-\beta_1)z_i(t-1) \tag{3}$$

$$A_m[n_i(t+1)] = (1-\beta_2)A_m[n_i(t)] \tag{4}$$

$$\eta_i(t) = \begin{cases} 0, & t = 0 \\ +\left|n_i(t-1)\right|, & t > 0, \quad u_i(t) < u_i(t-1) \\ -\left|n_i(t-1)\right|, & t > 0, \quad u_i(t) \geq u_i(t-1) \end{cases} \tag{5}$$

where u_i is the input of neuron i, v_i is the output of neuron i; k is the damping factor of the nerve membrane; α is the scaling parameter of neuron; w_{ij} is the connection weight from neuron j to neuron i; b_i is the input bias of neuron i; $z_i(t)$ is the self-feedback connection weight of neuron i; I_0 is a positive parameter; $n_i(t)$ is the stochastic noise added

to neuron i, which follows the uniform distribution of $[-A_m, A_m]$, and A_m is the amplitude of $n_i(t)$; β_2 is the damping factor of A_m, $0<\beta_2<1$; ε is the steepness parameter of the activation function; β_1 is the damping factor of $z_i(t)$, $0<\beta_1<1$; $\eta_i(t)$ is a temporary variable, $|n_i(t-1)|$ represents the absolute value of $n_i(t-1)$.

HNCNN is able to exhibit both hysteretic dynamics and stochastic chaotic simulated annealing properties without adding additional system parameters [19]. From the dynamical model of the network, it can be seen that the hysteresis properties of the network are generated by the controlled noise in the manner specified in equation (5), and from equations (2) and (5) the activation function consists of two biased sigmoid functions and produces a hysteresis loop [25].

B. ENERGY FUNCTION

In [23], we proposed a novel energy function for solving DCA for large-scale cellular networks, which is described as

$$\begin{aligned} E = {} & \frac{A_e}{2}\sum_{x=1}^{m}\sum_{i=1}^{n}\sum_{j\neq i} v_{xi}v_{xj}f_{CSC}(i,j) \\ & + \frac{B_e}{2}\sum_{x=1}^{m}\sum_{i=1}^{n}\sum_{\substack{y\in Near\\ y\neq x}}\sum_{j\neq i} v_{xi}v_{yj}f_{AFC}(i,j) \\ & + \frac{C_e}{2}\sum_{x=1}^{m}\sum_{i=1}^{n}\sum_{y\neq x} v_{xi}v_{yi}f_{CFC}(x,y) + \frac{D_e}{2}\sum_{x=1}^{m}\left(\sum_{i=1}^{n} v_{xi} - R_x\right)^2 \\ & + F_e\sum_{x=1}^{m}\sum_{i=1}^{n} v_{xi}T_{xi} + G_e\sum_{x=1}^{m}\sum_{i=1}^{n} iv_{xi} \end{aligned} \tag{6}$$

where x, y represent serial numbers of different cells, and i, j represent serial numbers of different available frequencies; m is the total number of cells in a CRCN, and n is the total number of available frequencies; v_{xi} represents output of the x_i^{th} neuron, whose value is 1 ($v_{xi}=1$) if frequency i is assigned to cell x, 0 otherwise.

The first term of (6) represents CSC, where product $v_{xi}v_{xj}$ indicates that frequencies i and j (j is not equal to i) are assigned to cell x simultaneously. Only when the constraint function $f_{\mathrm{CSC}}(i,j)=0$ is the first term equal to 0.

The CSC constraint function is defined as

$$f_{\mathrm{CSC}}(i,j) = \begin{cases} 1, & |i-j| < L \\ 0, & |i-j| \geq L \end{cases} \tag{7}$$

where L is the interval of frequencies i and j; $|i\text{-}j|$, the span of frequencies i and j.

The second term represents AFC, where product $v_{xi}v_{yj}$ indicates that frequencies i and j (j is not equal to i) are simultaneously assigned to cells x and y (y is not equal to x, and y is the neighboring cell of cell x), respectively. Only when the constraint function $f_{\mathrm{AFC}}(i,j)=0$ is the second term equal to 0. The denotation *Near* in the second term is the set of neighboring cells of cell x.

The AFC constraint function is defined as

$$f_{AFC}(i,j) = \begin{cases} 1, & |i-j| < 2 \\ 0, & |i-j| \geq 2 \end{cases} \tag{8}$$

The third term represents CFC, where product $v_{xi}v_{yi}$ indicates that frequency i is assigned to cells x and y (y is not equal to x) simultaneously. Only when the constraint function $f_{\mathrm{CFC}}(x,y)=0$ is the third term equal to 0.

The CFC constraint function is defined as

$$f_{CFC}(x,y) = \begin{cases} 1, & |x-y| < D_{reuse} \\ 0, & |x-y| \geq D_{reuse} \end{cases} \tag{9}$$

where D_{reuse} is the reuse distance between two cells which can be assigned the same frequencies [23].

The fourth term represents the frequency requirement constraint of each cell. When the total number of frequencies allocated in cell x equals the number of frequencies required by cell x, its value will reach 0, expressed as R_x. The number of required frequencies of all cells makes up the frequency requirement vector denoted by $\boldsymbol{R}$, R_x is the x^{th} element of $\boldsymbol{R}$.

The penultimate term represents the interference constraint between a CRCN and PUs, and its value will increase if frequency i is forbidden for cell x (occupied by PUs), otherwise, it is 0. T_{xi} is the x_i^{th} element of interference frequencies table $\boldsymbol{T}$, product $v_{xi}T_{xi}$ represents that either v_{xi} or T_{xi} is equal to 0, its product equals to 0.

The last term represents the rule of frequency compaction, and it will reach a positive constant which cannot be predicted even if HNCNN converges to an optimal solution. iv_{xi} is the product of frequency serial number i and the x_i^{th} neuron output v_{xi}, it means that the lower serial number of frequency i is allocated to cell x, the smaller value of (6) is obtained. When (6) is minimized, the total number of the assigned frequencies is the least, then the spectrum utilization is the highest.

The positive constants A_e, B_e, C_e, D_e, F_e, and G_e in (6) are corresponding penalty parameters that can be adjusted independently based on the convergence performance of HNCNN.

C. MOTION EQUATION OF HNCNN

Based on (6), the motion equation of HNCNN can be deduced as

$$\begin{aligned} \frac{du_{xi}}{dt} = {} & -\frac{\partial E}{\partial v_{xi}} = -A_e\sum_{j\neq i} v_{xj}f_{CSC}(i,j) \\ & - B_e\sum_{\substack{y\in Near\\ y\neq x}}\sum_{j\neq i} v_{yj}f_{AFC}(i,j) \\ & - C_e\sum_{y\neq x} v_{yi}f_{CFC}(x,y) - D_e\left(\sum_{j=1}^{n} v_{xj} - R_x\right) \\ & - F_eT_{xi} - G_ei \end{aligned} \tag{10}$$

where u_{xi} is the internal state of the x_i^{th} neuron, and the relationship of $v_{xi}(t)$ and $u_{xi}(t)$ is defined as that of v_i and u_i

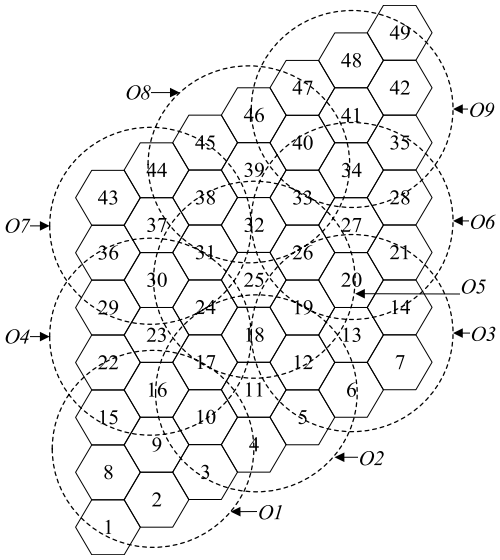

FIGURE 1. A 49-cell CRCN with 70 licensed frequencies in which nine being occupied by PUs.

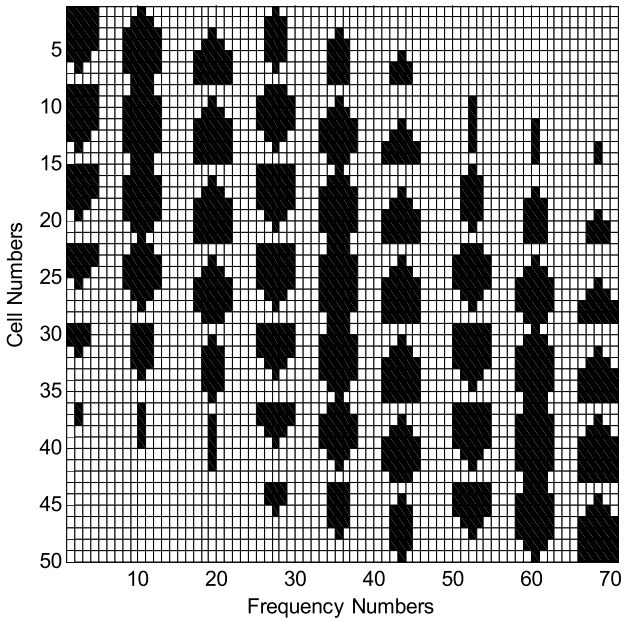

FIGURE 2. Interference frequency table of the 49-cell CRCN.

in (2).

$$\begin{aligned} u_{xi}(t+1) = {} & k u_{xi}(t) - A_e \alpha \sum_{j \neq i} v_{xj}(t) f_{CSC}(i,j) \\ & - B_e \alpha \sum_{\substack{y \in Near \\ y \neq x}} \sum_{j \neq i} v_{yj}(t) f_{AFC}(i,j) \\ & - C_e \alpha \sum_{y \neq x} v_{yi}(t) f_{CFC}(x,y) \\ & - D_e \alpha \left(\sum_{j=1}^{n} v_{xj}(t) - R_x \right) \\ & - \alpha F_e T_{xi} - \alpha G_e i - z_{xi}(t) \left[v_{xi}(t) - I_0 \right] + n_{xi}(t) \end{aligned} \tag{11}$$

where the simulated annealing function of $z_{xi}(t)$ is defined as that of $z_i(t)$ in (3); damping stochastic noise $n_{xi}(t)$ is defined as $n_i(t)$ in (4); the other symbols are the same as those in the aforementioned equations.

III. APPLICATION EXAMPLES

The application examples are based on a 49-cell CRCN. The simulation is accomplished using MATLAB.

A. VALIDITY OF THE ENERGY FUNCTION

A 49-cell CRCN with 70 licensed frequencies is illustrated in Fig. 1. Each cell has equal opportunities to be assigned one or more vacant frequencies from the 70 licensed frequencies. The cells in the CRCN are numbered from 1 to 49 (figures in each cell), which form a parallelogram pattern.

In Fig. 1, reuse distance D_{reuse} in (9) is defined as the distance between cells 1 and 16. Any two cells whose distance is greater than or equal to D_{reuse} may be assigned the same frequencies. The interval of frequencies of (7) is set as $L = 3$. There are nine rings noted as $O1$ to $O9$, which represent nine frequencies coverage regions occupied by PUs. We assume that frequencies 2, 10, 19, 27, 35, 43, 52, 60, and 68 are occupied by PUs in regions $O1$ to $O9$, respectively. The corresponding interference frequency table of Fig. 1 is shown in Fig. 2, which is calculated by the central server.

In Fig. 2, a black grid represents that a frequency is forbidden for a cell, whereas a blank grid represents a vacant one.

For example, in region $O2$, frequency 10 is occupied by PUs in cells 3, 4, 5, 6, 9, 10, 11, 12, 13, 16, 17, 18, 19, 23, 24, and 25. In order to avoid causing harmful interference to PUs, the three interference constraints should be taken into account. As a result, frequencies 8, 9, 11, and 12 are forbidden for cells 3, 4, 5, 6, 9, 10, 11, 12, 13, 16, 17, 18, 19, 23, 24, and 25 (CSC is satisfied); frequencies 9 and 11 are forbidden for cells 2, 7, 8, 14, 15, 20, 22, 26, 29, 30, 31, and 32 (AFC is satisfied); frequency 10 is forbidden for cells 1, 2, 7, 8, 14, 15, 20, 21, 22, 26, 27, 29, 30, 31, 32, 33, 36, 37, 38, and 39 (CFC is satisfied). The occupied frequency 10 and its related three interference constraints make up of the interference frequencies of region $O2$, which is shown in columns 8, 9, 10, 11, and 12. It is the same rule to other regions.

The DFA process for CRCN should avoid the interference frequencies in Fig. 2, *i.e.* the black grids. In addition, DFA should also avoid causing mutual interference among cells, *i.e.* the three interference constraints mentioned in (7), (8), (9).

Based on the 49-cell CRCN, we use the same HNCNN parameters as [23] to run HNCNN for a uniform frequency requirement to verify the proposed energy function.

A uniform assigned frequency table (*i.e.*, each cell is assigned an equal number of frequencies) for the 49-cell CRCN is shown in Fig. 3, where four frequencies per cell are assigned ($R_x = 4, x = 1, 2, \ldots, 48, 49$). A black grid means

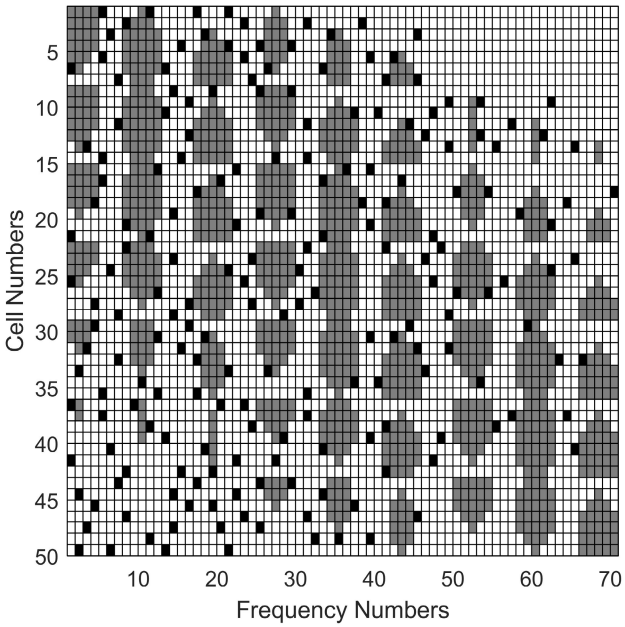

FIGURE 3. Uniform frequency assignment for the 49-cell CRCN with frequency compaction.

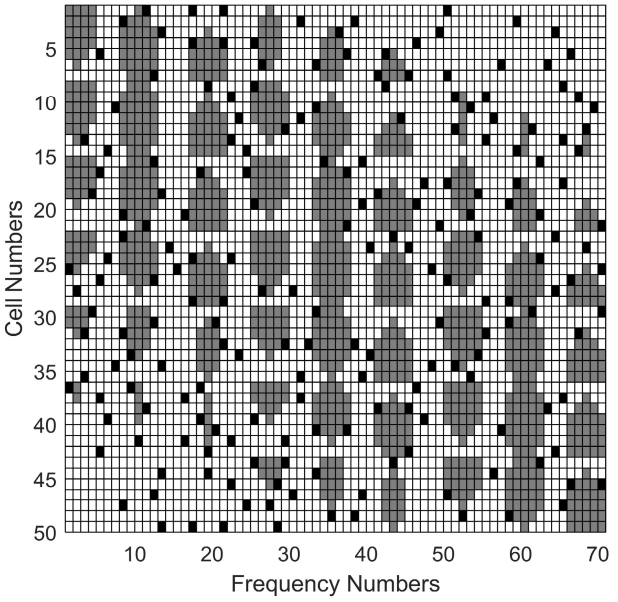

FIGURE 4. Uniform frequency assignment for the 49-cell CRCN without frequency compaction.

that a frequency is assigned to a cell, whereas a blank grid represents a vacant one. The gray grids shown in Fig. 3 (and the following Fig. 4 and 5) are originated from Fig. 2, which represent the interference frequency table. That is to say, the gray grids shown in Fig. 3, 4 and 5 are actually the same with the black grids shown in Fig. 2.

In Fig. 3, it can be easily seen that all frequencies assigned in a cell keep at least 3 intervals in the frequency domain (CSC is satisfied), every two frequencies assigned in the neighboring cells keep at least 2 intervals in the frequency domain (AFC is satisfied), all cells assigned the same frequency keep a distance greater than or equal to the reuse distance (CFC is satisfied). By comparing Fig. 3 with Fig. 2, the interference frequencies in Fig. 2 are all avoided in Fig. 3. That is to say, The gray and black grids in Fig. 3 do not overlap with each other.

Another satisfactory result in Fig. 3 is that the assigned frequencies are converged to lower serial numbers, which is caused by the last term of (6). As the serial number increases, the assigned times for a frequency are gradually decreased. For example, frequencies 66 and 70 are only assigned once, and frequencies 67, 68, and 69 are never assigned. This means that a frequency with a lower serial number has a higher priority to be assigned. As a result, the total number of the assigned frequencies becomes smaller, *i.e.*, the spectrum utilization is improved.

To verify the frequency compaction term in (6), we set the last punishing parameter as $G_e = 0$, whereas the other parameters remain unchanged. The corresponding assigned frequency table without frequency compaction is shown in Fig. 4. In this case, each cell still obtains four frequencies, but each frequency has equal opportunities to be assigned.

In a cell, all SUs are controlled by the BS, so the common control channel should be relatively fixedly assigned to each cell. However, DFA for CRCN using HNCNN is a centralized assignment scheme, a DFA process will probably cause plenty of frequency reassignments, which refer to the switching of many ongoing SUs to other frequencies in order to vacate available frequencies for incoming SUs, *i.e.*, to find a global optimal solution. In order to relatively fixedly assign a frequency to a cell as the dedicated common control channel, a feasible scheme is to select a frequency with the lowest serial number from the assigned frequencies, and it should not be switched as long as it is not occupied by PUs. Furthermore, the lowest-number frequency is easy to be found by new arrival SUs in a cell.

According to the above rules, we simply add the lowest-number frequencies with three interference constraints to the interference frequency table. As a result, the interference frequency table not only contains the frequencies occupied by PUs, but also contains the frequencies for the common control channels. After that, we implement HNCNN for the remanent frequencies requirement (without the lowest-number frequencies) of each cell. In Fig. 3, the lowest-number frequencies in the 49 cells are 5, 8, 6, 15, 5, 1, 7, 14, 16, 13, 7, 16, 3, 5, 12, 5, 17, 4, 14, 8, 1, 8, 14, 6, 1, 12, 4, 7, 4, 12, 3, 17, 2, 10, 5, 1, 5, 11, 13, 6, 1, 8, 7, 2, 4, 8, 3, 11, and 2. We assume that cell 10 must be assigned five frequencies, and the other cells are still assigned four frequencies. The assigned frequency table is shown in Fig. 5.

In Fig. 5, except cell 10, the other cells are still assigned four frequencies. Compared with Fig. 3, it is found that the lowest-number frequencies in each cell are unchanged, whereas many other frequencies are switched. The other features of Fig. 5 are the same as those of Fig. 3.

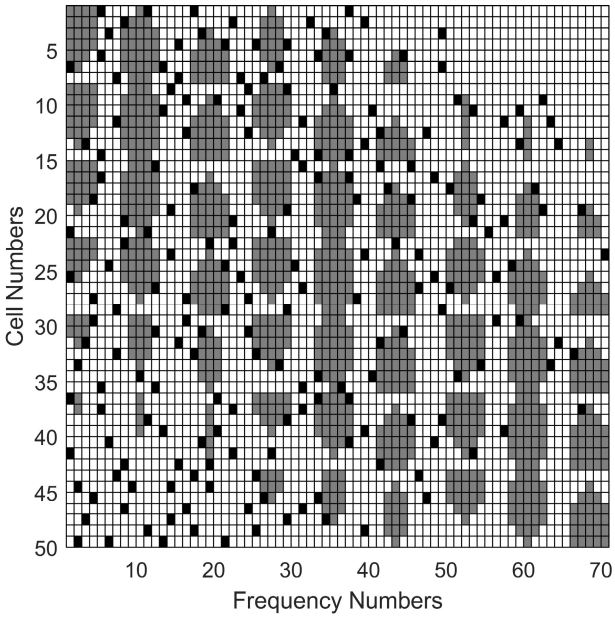

FIGURE 5. Frequency assignment with fixed common control channel.

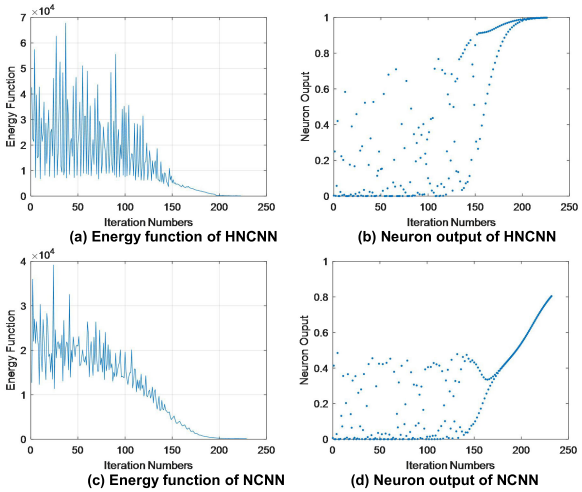

FIGURE 6. Energy function and neuron output of HNCNN and NCNN.

If one or more lowest-number frequency is occupied by PUs, then update the interference frequency table, and implement DFA process once again. So the lowest-number frequencies are reassigned.

B. EFFICIENCY OF HNCNN

In order to compare the efficiency of HNCNN and NCNN, we describe their respective energy function and the output of neuron in Fig. 6(a)-(d). The neuron output graph is randomly selected from No. (24,15) neuron, *i.e.,* $v_{24,15}(t)$.

It can be seen from Fig. 6(a) and (b) that when HNCNN is in the chaotic state of hysteretic noise within about 150 iterations, the energy function and neuron output curve fluctuate greatly, which is caused by the decaying random noise. In Fig. 6(b), the search space of HNCNN is expanded to about 0.9, which is conducive to improving the search probability

TABLE 1. Rate of the optimal solution of NCNN and HNCNN.

ALGORITHM	CELL	FREQUENCY PER CELL				
		1	2	3	4	5
HNCNN	49	100%	100%	100%	98%	95%
NCNN	49	100%	100%	95%	92%	87%

of the optimal solution. After about 160 iterations, the energy function and neuron output gradually converge to a fixed point. The average number of iterations is about 200.

In contrast, Fig. 6(c) and (d) show that within about 150 iterations, the search space of NCNN in the noise chaotic dynamics stage is approximately 0.5. It is worth noting that when both HNCNN and NCNN are within 150 iterations, the search space of HNCNN is 0.4 more than that of NCNN. This is due to the introduction of hysteretic excitation function into noisy chaotic neural network. Hysteretic chaotic neurons have certain ability to suppress noise [26]. Hysteresis dynamics can make neurons have faster change speed, can quickly escape from the original state of neurons, and also has the ability to overcome the network falling into local minima [27]. After about 200 iterations of NCNN, the energy function and neuron output will gradually converge to a fixed point. The last point is that the energy function curves of both HNCNN and NCNN will converge to zero. This is because we set the last punishing parameter to Ge=0 for ease of observation and for statistical the rate of optimal solutions.

In order to accurately evaluate the efficiency of HNCNN and NCNN, we implemented HNCNN and NCNN for 49 CRCN based on the interference frequency table shown in Fig. 2, and compared their efficiency. All cells are assigned from 1 to 5 frequencies on the average. Each case is simulated 100 times, and the results are summarized in Table 1.

In Table 1, the rates of optimal solution of HNCNN and NCNN decrease as the average frequency requirement increases. When the average frequency requirement is one or two, the rates of optimal solutions are both 100%, and when the average frequency requirement is over two, the rate of optimal solutions of HNCNN is significantly better than that of NCNN. A frequency requirement over 5 frequencies per cell has not been found by either HNCNN or NCNN based on Fig. 2.

IV. CONCLUSION

CRCN is a promising wireless access paradigm for cognitive radio. However, the available frequencies (unoccupied by PUs) for a CRCN are not fixed and constantly change over time from one region to another. So the DFA problem for a CRCN becomes more complicated than DCA for traditional cellular networks. To find a feasible scheme of DFA for CRCNs is a highly influential work for the future cognitive radio.

In this paper, a novel DFA technique for CRCNs using HNCNN is presented, in which an existing energy function is introduced to assign the required frequencies to each cell, and simultaneously avoid causing harmful interference to PUs and mutual interference among cells. In addition, in order to

relatively fixedly assign a common control channel to each cell, an assigned frequency with the lowest serial number is fixed until it is occupied by PUs. The simulation results of 49-cell CRCN show that the rate of optimal solution of HNCNN is significantly better than that of NCNN. Compared to NCNN, HNCNN exhibits better effective convergence of the optimal solution at higher noise levels, and has a wider search space.

In this paper, we only consider the small-scale CRCN with 49 cells. However, similar to large-scale cellular network (LCN) [23], a practical CRCN is also large scale with hundreds or even thousands of cells. Therefore, it still remains a problem that how to solve the DFA problem for a practical large-scale CRCN. A feasible scheme is to decompose a large-scale CRCN into many small-scale subnets. The DFA process is simply implemented in each subnet independently according to the interference information of its neighboring subnets.

ACKNOWLEDGMENT

The authors would like to thank the reviewers for their constructive comments. They appreciate the essential help from the College of Electronic Information and the College of Petroleum Engineering, Yangtze University.

REFERENCES

[1] C. Cordeiro, K. Challapali, D. Birru, and S. Shankar, "IEEE 802.22: The first worldwide wireless standard based on cognitive radios," in *Proc. 1st IEEE Int. Symp. New Front. Dyn. Spectr. Access Netw. (DySPAN)*, Nov. 2005, pp. 328–337.

[2] J. Mitola and G. Q. Maguire, "Cognitive radio: Making software radios more personal," *IEEE Pers. Commun.*, vol. 6, no. 4, pp. 13–18, Aug. 1999.

[3] K. Hsieh, F. Tseng, and M. Ku, "A spectrum and energy cooperation strategy in hierarchical cognitive radio cellular networks," *IEEE Wireless Commun. Lett.*, vol. 5, no. 3, pp. 252–255, Jun. 2016.

[4] S. Haykin, "Cognitive radio: Brain-empowered wireless communications," *IEEE J. Sel. Areas Commun.*, vol. 23, no. 2, pp. 201–220, Feb. 2005.

[5] I. F. Akyildiz, W.-Y. Lee, M. C. Vuran, and S. Mohanty, "A survey on spectrum management in cognitive radio networks," *IEEE Commun. Mag.*, vol. 46, no. 4, pp. 40–48, Apr. 2008.

[6] A. Goldsmith, S. A. Jafar, I. Maric, and S. Srinivasa, "Breaking spectrum gridlock with cognitive radios: An information theoretic perspective," *Proc. IEEE*, vol. 97, no. 5, pp. 894–914, May 2009.

[7] J. Jia, Q. Zhang, and X. Shen, "HC-MAC: A hardware-constrained cognitive MAC for efficient spectrum management," *IEEE J. Sel. Areas Commun.*, vol. 26, no. 1, pp. 106–117, Jan. 2008.

[8] D. Niyato and E. Hossain, "Cognitive radio for next-generation wireless networks: An approach to opportunistic channel selection in IEEE 802.11-based wireless mesh," *IEEE Wireless Commun.*, vol. 16, no. 1, pp. 46–54, Feb. 2009.

[9] Y. Ma, D. I. Kim, and Z. Wu, "Optimization of OFDMA-based cellular cognitive radio networks," *IEEE Trans. Commun.*, vol. 58, no. 8, pp. 2265–2276, Aug. 2010.

[10] L. Sboui, H. Ghazzai, Z. Rezki, and M. Alouini, "On green cognitive radio cellular networks: Dynamic spectrum and operation management," *IEEE Access*, vol. 4, pp. 4046–4057, 2016.

[11] S. H. R. Bukhari, M. H. Rehmani, and S. Siraj, "A survey of channel bonding for wireless networks and guidelines of channel bonding for futuristic cognitive radio sensor networks," *IEEE Commun. Surveys Tuts.*, vol. 18, no. 2, pp. 924–948, 2nd Quart., 2016.

[12] D. Kunz, "Channel assignment for cellular radio using neural networks," *IEEE Trans. Veh. Technol.*, vol. 40, no. 1, pp. 188–193, Feb. 1991.

[13] P. L. Hiew and M. Zukerman, "Efficiency comparison of channel allocation schemes for digital mobile communication networks," *IEEE Trans. Veh. Technol.*, vol. 49, no. 3, pp. 724–733, May 2000.

[14] A. Hoang and Y.-C. Liang, "A two-phase channel and power allocation scheme for cognitive radio networks," in *Proc. IEEE 17th Int. Symp. Pers., Indoor Mobile Radio Commun.*, Sep. 2006, pp. 1–5.

[15] Y. Chen, N. Han, S. Shon, and J. Kim, "Dynamic frequency allocation based on graph coloring and local bargaining for multi-cell WRAN system," in *Proc. Asia–Pacific Conf. Commun.*, Aug. 2006, pp. 1–5.

[16] R. Ahmed, Y. Chen, B. Hassan, and L. Du, "CR-IoTNet: Machine learning based joint spectrum sensing and allocation for cognitive radio enabled IoT cellular networks," *Ad Hoc Netw.*, vol. 112, Mar. 2021, Art. no. 102390.

[17] J.-S. Kim, S. Ho Park, P. W. Dowd, and N. M. Nasrabadi, "Cellular radio channel assignment using a modified Hopfield network," *IEEE Trans. Veh. Technol.*, vol. 46, no. 4, pp. 957–967, Nov. 1997.

[18] Z. He, Y. Zhang, C. Wei, and J. Wang, "A multistage self-organizing algorithm combined transiently chaotic neural network for cellular channel assignment," *IEEE Trans. Veh. Technol.*, vol. 51, no. 6, pp. 1386–1396, Nov. 2002.

[19] M. Sun, L. Zhao, W. Cao, Y. Xu, X. Dai, and X. Wang, "Novel hysteretic noisy chaotic neural network for broadcast scheduling problems in packet radio networks," *IEEE Trans. Neural Netw.*, vol. 21, no. 9, pp. 1422–1433, Sep. 2010.

[20] L. Wang, S. Li, F. Tian, and X. Fu, "A noisy chaotic neural network for solving combinatorial optimization problems: Stochastic chaotic simulated annealing," *IEEE Trans. Syst., Man, Cybern., B, Cybern.*, vol. 34, no. 5, pp. 2119–2125, Oct. 2004.

[21] L. Chen and K. Aihara, "Chaotic simulated annealing by a neural network model with transient chaos," *Neural Netw.*, vol. 8, no. 6, pp. 915–930, 1995.

[22] J. J. Hopfield and D. W. Tank, "'Neura' computation of decisions in optimization problems," *Biol. Cybern.*, vol. 52, no. 3, pp. 141–152, Jul. 1985.

[23] C. Zhao and L. Gan, "Dynamic channel assignment for large-scale cellular networks using noisy chaotic neural network," *IEEE Trans. Neural Netw.*, vol. 22, no. 2, pp. 222–232, Feb. 2011.

[24] M. Sun, K. Zhai, W. Cao, Y. Wang, and Y. Xu, "Hybrid OFDMA resource allocation scheme for ensuring required level of proportional fairness," *Math. Problems Eng.*, vol. 2020, pp. 1–19, Oct. 2020.

[25] M. Sun, K. Y. Lee, Y. Xu, and W. Bai, "Hysteretic noisy chaotic neural networks for resource allocation in OFDMA system," *IEEE Trans. Neural Netw. Learn. Syst.*, vol. 29, no. 2, pp. 273–285, Feb. 2018.

[26] J. Qiao, Z. Hu, and W. Li, "Hysteretic noisy frequency conversion sinusoidal chaotic neural network for traveling salesman problem," *Neural Comput. Appl.*, vol. 31, no. 11, pp. 7055–7069, Nov. 2019.

[27] M. Sun, Y. Huang, S. Wang, and Y. Xu, "Novel bee colony optimization with update quantities for OFDMA resource allocation," *Wireless Commun. Mobile Comput.*, vol. 2021, pp. 1–14, Jul. 2021.

CHENGZHI ZHAO was born in Hubei, China, in 1973. He received the M.S. and Ph.D. degrees in electrical engineering from Wuhan University, Hubei, in 2005 and 2011, respectively.

He is currently a Lecturer with Yangtze University, Hubei. His current research interests include mobile communication, radio resource management, cognitive radio, and neural networks.

AO ZHANG was born in Hubei, China, in 1999. He is currently pursuing the master's degree with Yangtze University. His current research interests include artificial intelligence, cognitive radio, and mobile communication.